

(Security classification of title, body of abstract and indexed annotation must be entered when the overall report is classified)

1. ORIGINATING ACTIVITY (Corporate author)

GTE Sylvania Inc.

2a. REPORT SECURITY CLASSIFICATION

UNCLASSIFIED

2b. GROUP

3. REPORT TITLE

Infrared Photocathode

4. DESCRIPTIVE NOTES (Type of report and inclusive dates)

Annual Report

May 1 1971 - April 30 1972

5. AUTHOR(S) (Last name, first name, initial)

H. Sonnenberg

6. REPORT DATE

April 30, 1972

7a. TOTAL NO. OF PAGES

20

7b. NO. OF REFS

14

8a. CONTRACT OR GRANT NO.

N00014-70-C-0079

9a. ORIGINATOR'S REPORT NUMBER(S)

None

b. PROJECT NO.

9b. OTHER REPORT NO(S) (Any other numbers that may be assigned  
this report)

None

10. AVAILABILITY/LIMITATION NOTICES

Unlimited

11. SUPPLEMENTARY NOTES

None

12. SPONSORING MILITARY ACTIVITY

Advanced Research Projects Agency

13. ABSTRACT

The amount of Cs-0 low-work-function-surface material required to optimize the photoresponse of  $\text{InAs}_{0.4}\text{P}_{0.6}$  depends upon the wavelength at which the response is to be maximized. It is shown that the optimum thickness increases exponentially with wavelength.

The effect of thick Cs-0 layers on photoemission from GaAs and  $\text{InAs}_{0.4}\text{P}_{0.6}$  cathodes is experimentally investigated. Simple empirical relationships between the yield and thickness and between the escape probability and thickness are derived.

Reproduced by  
**NATIONAL TECHNICAL  
 INFORMATION SERVICE**  
 Springfield, Va. 22151

**BEST  
AVAILABLE COPY**

1A KEY WORDS	LINK A		LINK U		LINK C	
	ROLE	WT	ROLE	WT	ROLE	WT
Photoemission						
Photocathodes						
Cesium Oxide						
Heterojunctions						
Infrared Detector						

**INSTRUCTIONS**

1. **ORIGINATING ACTIVITY:** Enter the name and address of the contractor, subcontractor, grantee, Department of Defense activity or other organization (*corporate author*) issuing the report.
- 2a. **REPORT SECURITY CLASSIFICATION:** Enter the overall security classification of the report. Indicate whether "Restricted Data" is included. Marking is to be in accordance with appropriate security regulations.
- 2b. **GROUP:** Automatic downgrading is specified in DoD Directive 5200.10 and Armed Forces Industrial Manual. Enter the group number. Also, when applicable, show that optional markings have been used for Group 3 and Group 4 as authorized.
3. **REPORT TITLE:** Enter the complete report title in all capital letters. Titles in all cases should be unclassified. If a meaningful title cannot be selected without classification, show title classification in all capitals in parenthesis immediately following the title.
4. **DESCRIPTIVE NOTES:** If appropriate, enter the type of report, e.g., interim, progress, summary, annual, or final. Give the inclusive dates when a specific reporting period is covered.
5. **AUTHOR(S):** Enter the name(s) of author(s) as shown on or in the report. Enter last name, first name, middle initial. If military, show rank and branch of service. The name of the principal author is an absolute minimum requirement.
6. **REPORT DATE:** Enter the date of the report as day, month, year; or month, year. If more than one date appears on the report, use date of publication.
- 7a. **TOTAL NUMBER OF PAGES:** The total page count should follow normal pagination procedures, i.e., enter the number of pages containing information.
- 7b. **NUMBER OF REFERENCES:** Enter the total number of references cited in the report.
- 8a. **CONTRACT OR GRANT NUMBER:** If appropriate, enter the applicable number of the contract or grant under which the report was written.
- 8b, 8c, & 8d. **PROJECT NUMBER:** Enter the appropriate military department identification, such as project number, subproject number, system numbers, task number, etc.
- 9a. **ORIGINATOR'S REPORT NUMBER(S):** Enter the official report number by which the document will be identified and controlled by the originating activity. This number must be unique to this report.
- 9b. **OTHER REPORT NUMBER(S):** If the report has been assigned any other report numbers (*either by the originator or by the sponsor*), also enter this number(s).
10. **AVAILABILITY/LIMITATION NOTICES:** Enter any limitations on further dissemination of the report, other than those

imposed by security classification, using standard statements such as:

- (1) "Qualified requesters may obtain copies of this report from DDC."
- (2) "Foreign announcement and dissemination of this report by DDC is not authorized."
- (3) "U. S. Government agencies may obtain copies of this report directly from DDC. Other qualified DDC users shall request through \_\_\_\_\_."
- (4) "U. S. military agencies may obtain copies of this report directly from DDC. Other qualified users shall request through \_\_\_\_\_."
- (5) "All distribution of this report is controlled. Qualified DDC users shall request through \_\_\_\_\_."

If the report has been furnished to the Office of Technical Services, Department of Commerce, for sale to the public, indicate this fact and enter the price, if known.

11. **SUPPLEMENTARY NOTES:** Use for additional explanatory notes.
12. **SPONSORING MILITARY ACTIVITY:** Enter the name of the departmental project office or laboratory sponsoring (paying for) the research and development. Include address.
13. **ABSTRACT:** Enter an abstract giving a brief and factual summary of the document indicative of the report, even though it may also appear elsewhere in the body of the technical report. If additional space is required, a continuation sheet shall be attached.  
It is highly desirable that the abstract of classified reports be unclassified. Each paragraph of the abstract shall end with an indication of the military security classification of the information in the paragraph, represented as (TS), (S), (C), or (U).  
There is no limitation on the length of the abstract. However, the suggested length is from 150 to 225 words.
14. **KEY WORDS:** Key words are technically meaningful terms or short phrases that characterize a report and may be used as index entries for cataloging the report. Key words must be selected so that no security classification is required. Identifiers, such as equipment model designation, trade name, military project code name, geographic location, may be used as key words but will be followed by an indication of technical context. The assignment of links, rules, and weights is optional.

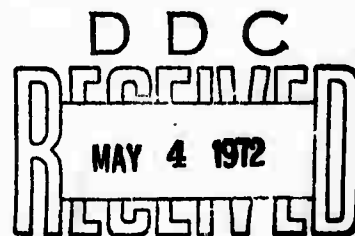
INFRARED PHOTOCATHODE  
ANNUAL TECHNICAL REPORT

AD 741260

ARPA Order Number:	1806
Program Code Number:	00014
Contractor:	GTE Sylvania Inc.
Effective Date:	1 November 1969
Expiration Date:	30 April 1972
Contract Amount:	\$178,686
Contract Number:	N00014-70-C-0079
Principal Investigator:	Dr. H. Sonnenberg
Telephone:	(415) 966-3472
Scientific Officer:	Dr. Robert E. Behringer

The views and conclusions contained in this document are those of the author and should not be interpreted as necessarily representing the official policies, either expressed or implied, of the Advanced Research Projects Agency or the U. S. Government.

Sponsored by  
Advanced Research Projects Agency  
ARPA Order No. 1806



Prepared by

Approved by

H. Sonnenberg  
H. Sonnenberg  
Electro-Optics Research and  
Development Department

R. S. Reynolds for  
L. M. Osterink, Manager  
Electro-Optics Research and  
Development Department

DISTRIBUTION STATEMENT A  
Approved for public release  
Distribution Unlimited

## TECHNICAL REPORT SUMMARY

The technical objective of this program is the development of an efficient photocathode for the 1.5 micron region of the infrared spectrum. No such photocathode exists today. The concept of the heterojunction photocathode proposed by us earlier<sup>(1)</sup>, represented a new approach to the development of an infrared cathode.

This approach, exploited on this contract, led to the discovery of the most efficient (at that time) 1.06 micron photocathode<sup>(2)</sup>. Further improvements in this cathode have been made, and even today it remains the most efficient 1.06 micron photocathode yet developed. Continued development of infrared cathodes on this project has led to photocathodes having, for the first time, usable response out to 1.3 microns, see Figure 3.

In Section 1.0 of this report we show that the "optimum thickness" of Cs-0 low-work-function surfaces used in processing heterojunction-type cathodes is wavelength dependent. A simple empirical relationship describing this dependence is derived. It is shown that the optimum thickness increases exponentially with wavelength. In Section 2 the effect of thick Cs-0 layers on photoemission from GaAs and InAs<sub>0.4</sub>P<sub>0.6</sub> cathodes is given. Simple empirical relationships between the yield and thickness and between the escape probability and thickness are derived. It is shown that the increased Cs-0 thickness required to optimize the infrared response of lower bandgap materials is in large part responsible for their lower photoresponse.

We have abandoned the simple "heterojunction" cathode approach in favor of an approach which provides for optical absorption in a small bandgap material which is in contact with a large bandgap material known to have a high electron escape probability.

(1) H. Sonnenberg, Appl. Phys. Letters 14 289 (1969).

(2) Quarterly Management Report #1 (Feb. 10, 1970); H. Sonnenberg, Applied Physics Letters 16, 245 (1970).

## Section 1

### WAVELENGTH DEPENDENCE OF OPTIMUM THICKNESS OF Cs-O LOW-WORK-FUNCTION SURFACES

In the Cs-O processing of a negative-electron-affinity-type infrared-photocathode one commonly finds that the photoresponse in the visible spectrum peaks earlier than the infrared response. Continued processing, beyond that required to optimize the visible response generally leads to continued improvement in the infrared response but at the expense of the response in the visible.<sup>(1)</sup> Thus for a given infrared cathode, different thicknesses of Cs-O low-work-function material are required to optimize the photoresponse at different wavelengths. We have investigated this behavior in detail for  $\text{InAs}_{0.4}\text{P}_{0.6}$ -(Cs-O) and report here a very simple empirical relationship between optimum thickness and wavelength.

$\text{InAs}_{0.4}\text{P}_{0.6}$  with a bandgap less than 1 eV was chosen since its useful photoresponse extends over a broad spectral range to 1.3 microns. The yield curves for different levels of Cs and  $\text{O}_2$  exposure were directly recorded with a phase-sensitive-detection apparatus and a Perkin-Elmer E-1 scanning monochromator. A complete scan from 0.45 microns to 1.4 microns takes about 15 minutes.

The photoresponse of the  $\text{InAs}_{0.4}\text{P}_{0.6}$  cathode with one monolayer of Cs<sup>(2)</sup> on the surface was first recorded. The simultaneous-exposure technique<sup>(1)</sup> was then used to process the cathode with Cs and  $\text{O}_2$  in approximately one-monolayer-of-Cs steps. The photoresponse at the end of each step was recorded.

To avoid Cs loss from the cathode between processing steps, the Cs channel, rather than being turned off completely, was turned down so that the arrival rate of Cs atoms at the cathode surface was in equilibrium with the loss rate. Stability in the photoresponse at each exposure level could easily be maintained this way.

To investigate the effect of increasing Cs-O coverage on the photoresponse of the cathode, the yield was plotted as a function of Cs exposure for different wavelengths as shown in Figure 1. Each vertical set of points represents the photoresponse of the cathode at that particular level of Cs and O<sub>2</sub> exposure. The first set of points (at 1.0 monolayers) is for Cs only, and subsequent sets of points are for increasing Cs-O exposure, measured in terms of Cs monolayers.

Figure 1 clearly shows that different thicknesses of Cs-O layers are required to optimize the photoresponse at different wavelengths. For example, the photoresponse at 4500Å is optimized by a coverage of only about 2.2 monolayers of Cs whereas the photoresponse at 10,500Å is not optimized until the coverage has grown to approximately 4.2 monolayers of Cs. (3)

The thickness corresponding to the maximum photoresponse (optimum thickness) at the different wavelengths is plotted in Figure 2 as a function of wavelength. The data points from 0.45 microns to 1.1 microns are taken from the position of the maxima of the parametric curves of Figure 1, whereas the points at 1.3 microns are taken from a number of different experiments where the processing was not interrupted until the response at 1.3 microns was optimized.

Figure 1 Quantum efficiency as a function of Cs-O low-work-function-surface thickness measured in monolayers of Cs, with wavelength as a parameter.

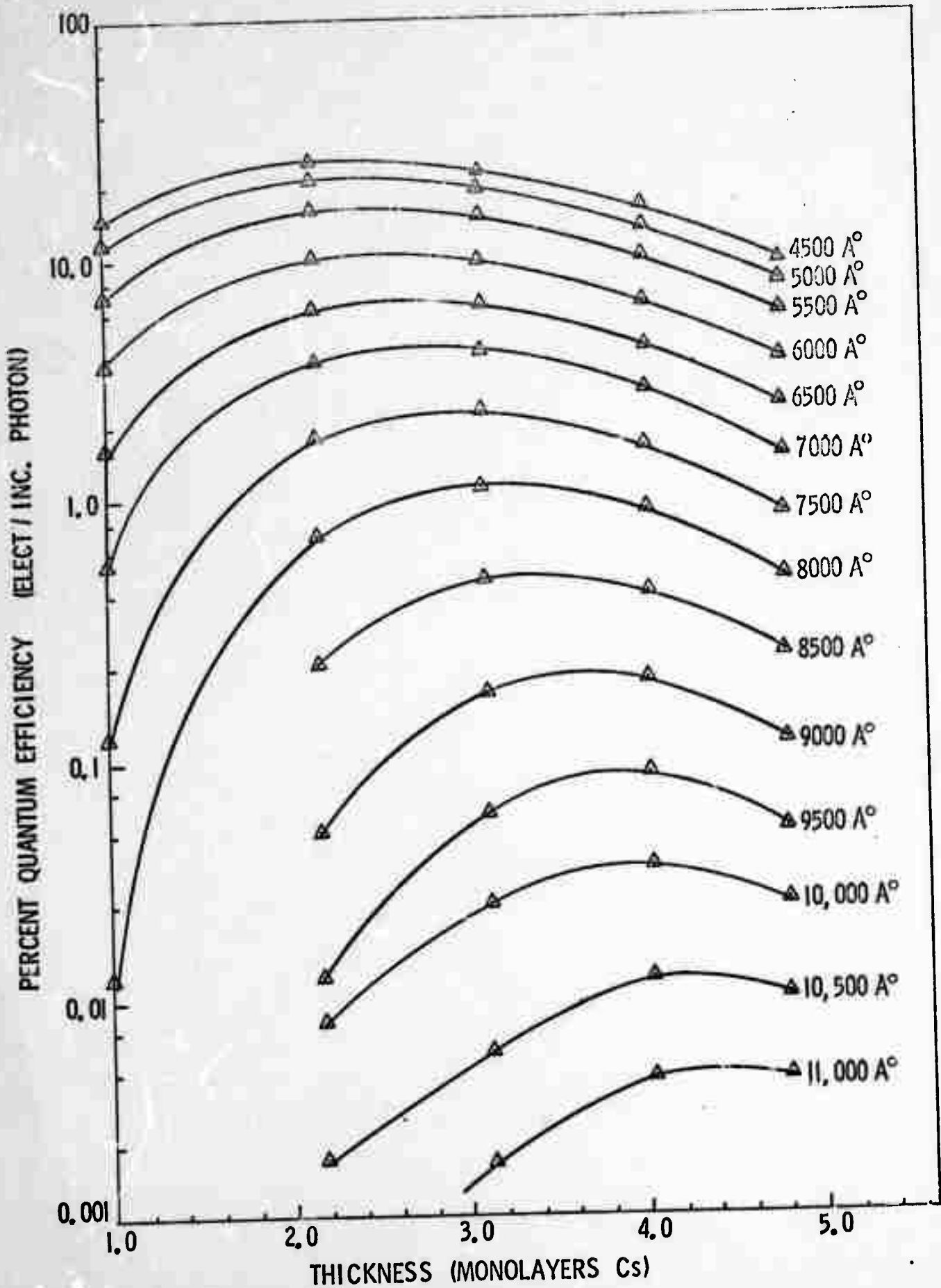
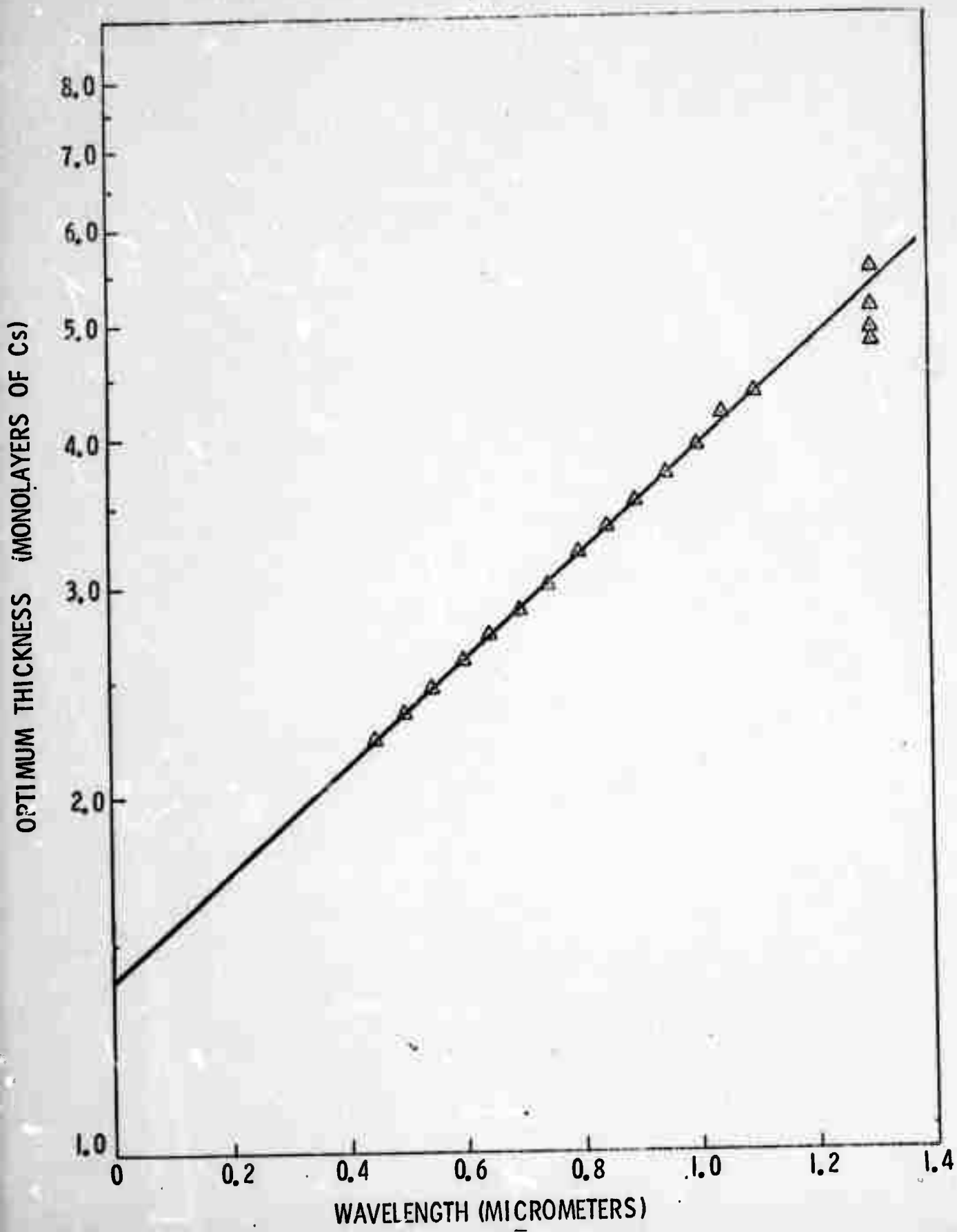


Figure 2 Thickness of Cs-O low-work-function surface required to maximize the photoresponse of  $\text{InAs}_{0.4}\text{P}_{0.6}$  as a function of wavelength.



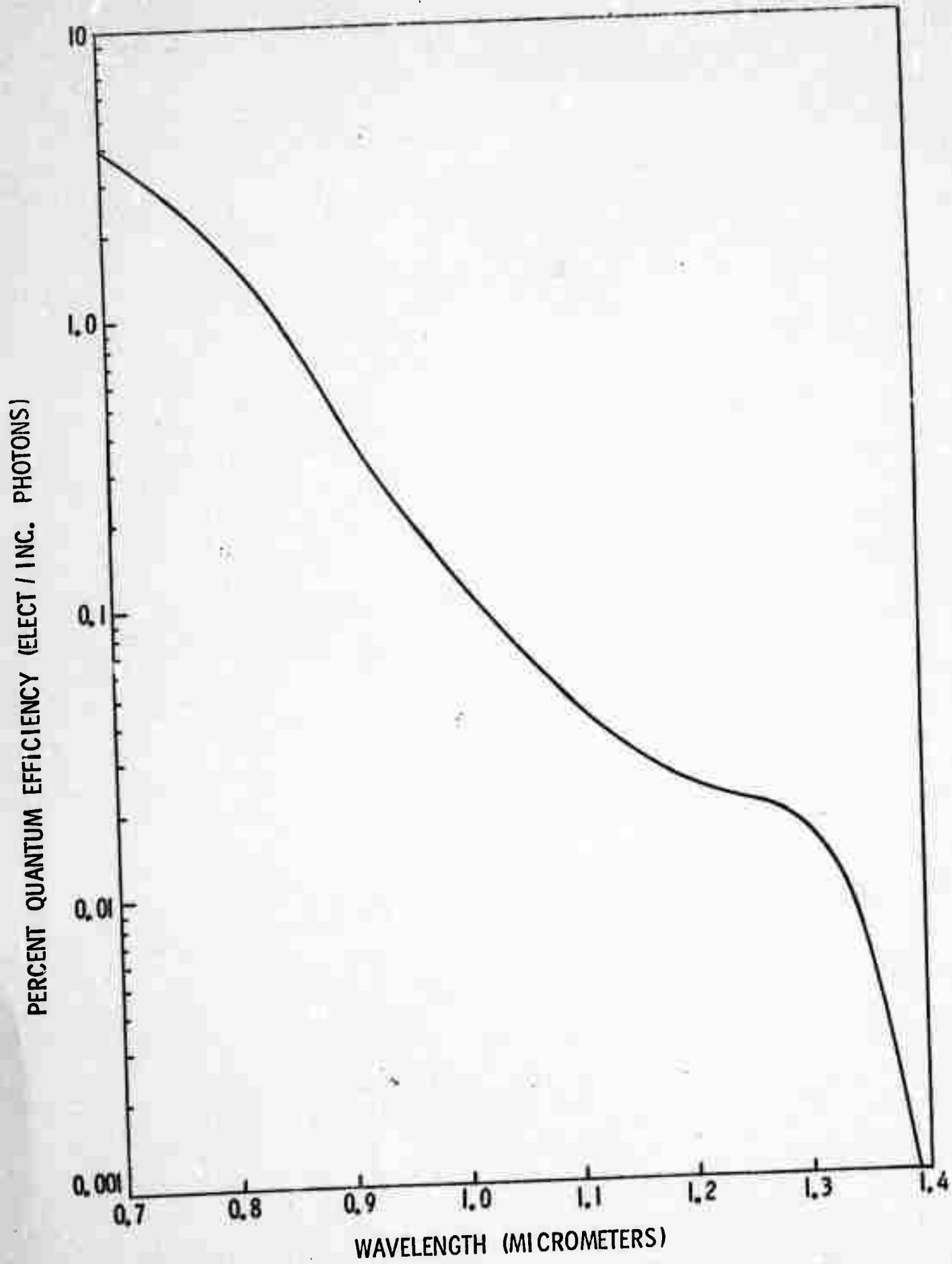
It is apparent from Figure 2 that the amount,  $t$ , of Cs-O (measured in monolayers of Cs) required to optimize the photoresponse is exponentially dependent on the wavelength,  $\lambda$  (micrometers) i.e.,

$$t = T e^{\beta\lambda} \quad (1)$$

For this particular experiment,  $T = 1.4$  monolayers of Cs<sup>(4)</sup> and  $\beta = 1.02$  micrometers<sup>-1</sup>. We have verified the exponential dependence for continuously processed cathodes as well. We find in general, however, that thinner Cs-O coverage is required to optimize the photoresponse of continuously processed cathodes, as demonstrated in Figure 2, and that the overall photoresponse of these cathodes is much better than that of cathodes for which the processing is interrupted. To underscore this, compare the yield curve shown in Figure 3 to the data at 4.8 monolayers shown in Figure 1. Figure 3 shows the spectral response<sup>(5)</sup> of the cathode represented by the point in Figure 2 at 1.3 microns and 4.9 monolayers of Cs<sup>(6)</sup>.

One may well ask if the exponential relationship given by equation (1) is applicable only to InAs<sub>0.4</sub>P<sub>0.6</sub> or if it is more universally applicable. Although we have not specifically attempted to determine the wavelength dependence of the optimum thickness for InAs<sub>0.25</sub>P<sub>0.75</sub>, the data that we do have are in agreement with equation (1). We have also attempted to verify equation (1) for GaAs. The parametric curves (comparable to those of Figure 1) exhibit a very broad maximum which makes interpretation difficult. If the optimum thickness for GaAs is exponentially dependent on the wavelength, then  $\beta$  is very small. It may be however, that equation (1), and this is purely conjecture, is applicable only to cathodes in which the top of the interfacial barrier is above the bottom of the conduction band.

Figure 3 Quantum yield of continuously-processed  $\text{InAs}_{0.4}\text{P}_{0.6}^{-}(\text{Cs-0})$



## Section 2

### EFFECT OF THICK Cs-O LAYERS ON PHOTOEMISSION FROM NEGATIVE-ELECTRON-AFFINITY CATHODES

The efficiency of small-bandgap-NEA cathodes near threshold is much less than the efficiency near threshold of larger-bandgap materials. For example, the yield of  $\text{InAs}_{0.4}\text{P}_{0.6}$  at 1.3 microns is only about  $10^{-3}$  that of GaAs at 0.85 microns. The major cause for this difference has been correctly indentified as due to interfacial-barrier effects<sup>(7,8)</sup>. However since thicker cesium-oxide coverage is required to optimize the photoresponse of smaller-bandgap materials<sup>(1)</sup>, part of the difference in threshold yield should be due to this difference in thickness. We have investigated the effect of thick Cs-O layers on photoemission from NEA cathodes and show that a substantial decrease in yield may be expected on the basis of the difference in thickness alone. A simple empirical relation giving the effect of thick Cs-O layers on photoemission is derived.

The yield data were directly recorded with an analog recording system which included a phase-sensitive-detection apparatus and a scanning monochromator. The  $\text{O}_2$  exposure was recorded with a partial pressure analyzer, and was used as a check on the Cs coverage<sup>(9)</sup> which was estimated by timing the exposure periods as described in reference 1. Photoemission measurements were made on GaAs and  $\text{InAs}_{0.4}\text{P}_{0.6}$ , sensitized with Cs and  $\text{O}_2$  by the simultaneous-exposure technique<sup>(1)</sup>.

The spectral response with the infrared yield optimized was first recorded. Additional yield curves were then recorded for increasing Cs and O<sub>2</sub> coverage. To avoid Cs loss from the cathode between processing steps, the Cs channel was turned down so that the arrival rate of Cs atoms at the cathode was in equilibrium with the loss rate. The point of equilibrium was estimated from the stability of the photoresponse and remained essentially the same at all exposure levels.

The quantum efficiency of GaAs at 7500Å is shown in Figure 4 as a function of thickness measured in monolayers<sup>(2)</sup> of Cs. The points represent the experimental values and the solid curve represents the equation

$$\eta = \eta_0 (1 - e^{-\ell/t}), \quad (2)$$

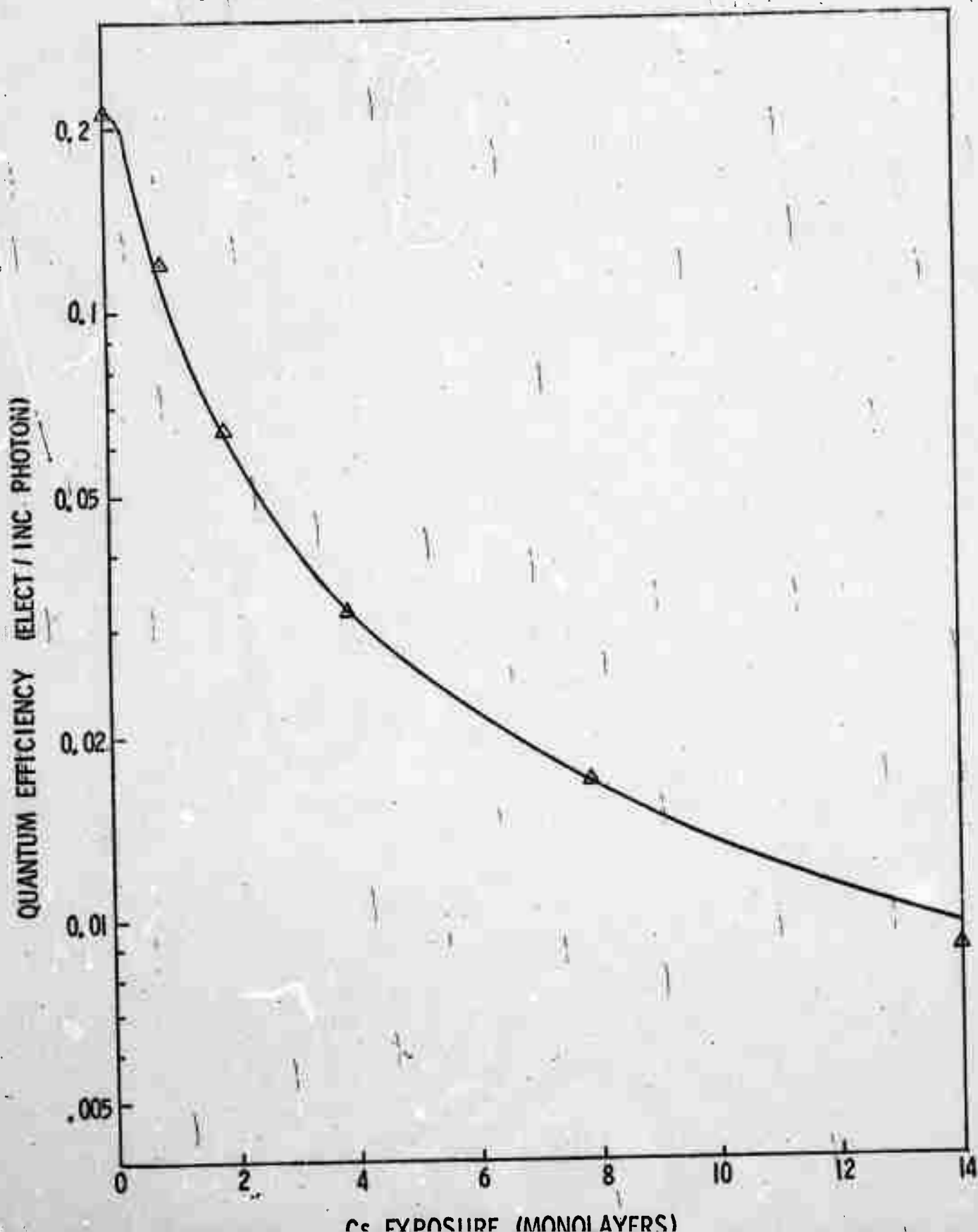
where  $\eta$  is the quantum efficiency (electrons/incident photon) as a function of thickness  $t$  (monolayers of Cs);  $\eta_0$  is the peak quantum efficiency (0.213 electrons/incident photon for the curve shown) and  $\ell$  (0.65 monolayers of Cs for the curve shown) is defined as the attenuation length. The thickness  $t$ , does not represent the total coverage but rather the coverage beyond that required to optimize the infrared photoresponse. The total coverage is given by  $t' = (t + t_0)$ , where  $t_0$  is the coverage required to optimize the infrared response.

Near threshold the yield of III-V NEA cathodes is given by (10)

$$\eta = P(1-R) F/[1 + (1/\alpha L)], \quad (3)$$

where the symbols used have the usual meaning. The factor  $F/[1 + (1/\alpha L)]$  which accounts for the generation and transport of the photoelectrons in the III-V semiconductor, clearly does not change with surface treatment. For the Cs-0

Figure 4 Thickness dependence of the quantum efficiency  $\eta$ , of GaAs at  $7500\text{\AA}$ . The points represent the experimental data and the solid curve is a plot of the equation  $\eta = 0.213(1 - e^{-0.65/t})$ .



layer thicknesses considered here, we can probably safely assume that the reflectivity  $R$  of the surface remains that of clean GaAs. This leaves only the escape probability  $P$ , dependent on surface treatment, which must therefore mirror the thickness dependence of  $\eta$ , i.e.,

$$P = P_0(1 - e^{-\ell/t}), \quad (4)$$

where  $P_0$  is the escape probability at  $t = 0$ . A similar argument will quickly show that equation (4) should be valid not only near threshold, but over the entire spectral range of response of the III-V NEA cathode.

To verify equation (4) experimentally we have made a least-squares-fit analysis of equation (3), and our yield data at each exposure level to determine  $P(t)$ . The points given in Figure 5 represent the escape probabilities at  $7500\text{\AA}$  obtained from the least-squares-fit analysis and the solid curve represents equation (4) with the escape probability<sup>(11)</sup>  $P_0 = 0.63$  and an attenuation length  $\ell = 0.65$  monolayers of Cs. As expected, the same attenuation length used to fit the data in Figure 4, describes the data in Figure 5. Equation 4 with  $P_0 = 0.57$  and  $L = 10$  "layers of Cs - 0" is also in reasonable agreement with the estimated X-electron-escape probability given in Figure 8 of Reference 12.

The attenuation length  $\ell$ , is not constant however, and Figure 6 shows its wavelength dependence. For the  $\Gamma$  electrons,  $\ell$  is approximately constant at 0.65 monolayers of Cs. We would expect a constant attenuation length for this case since most of the photoelectrons arriving at the surface have thermalized in the  $\Gamma$ -conduction-band minimum. At shorter wavelengths,  $\ell$  increases and appears to saturate at about 1.0 monolayer of Cs.

Figure 5 Thickness dependence of the escape probability P, of GaAs at 7500A. The points represent the experimental data and the solid curve is a plot of the equation  $P = 0.63(1 - e^{-0.65/t})$ .

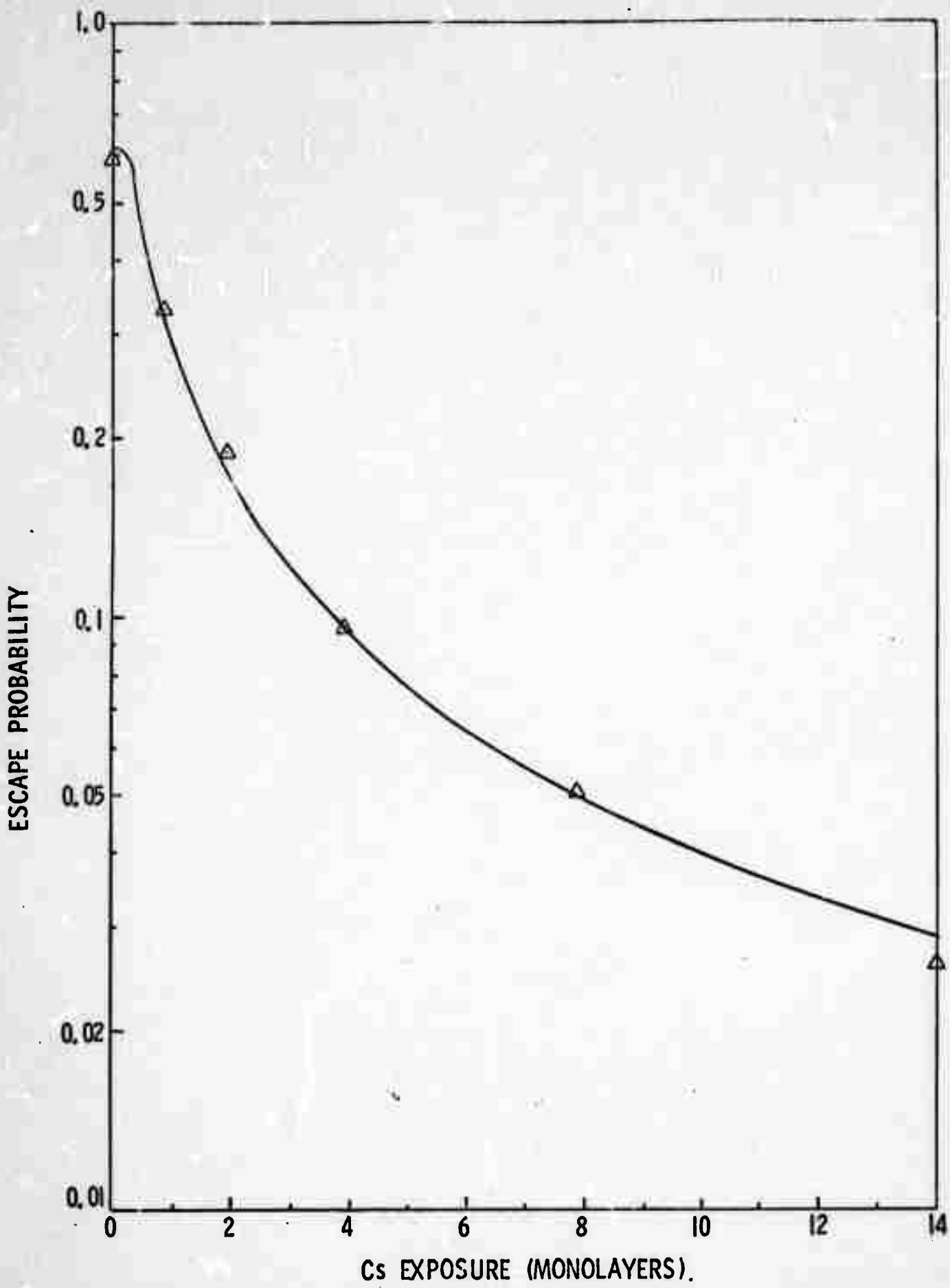
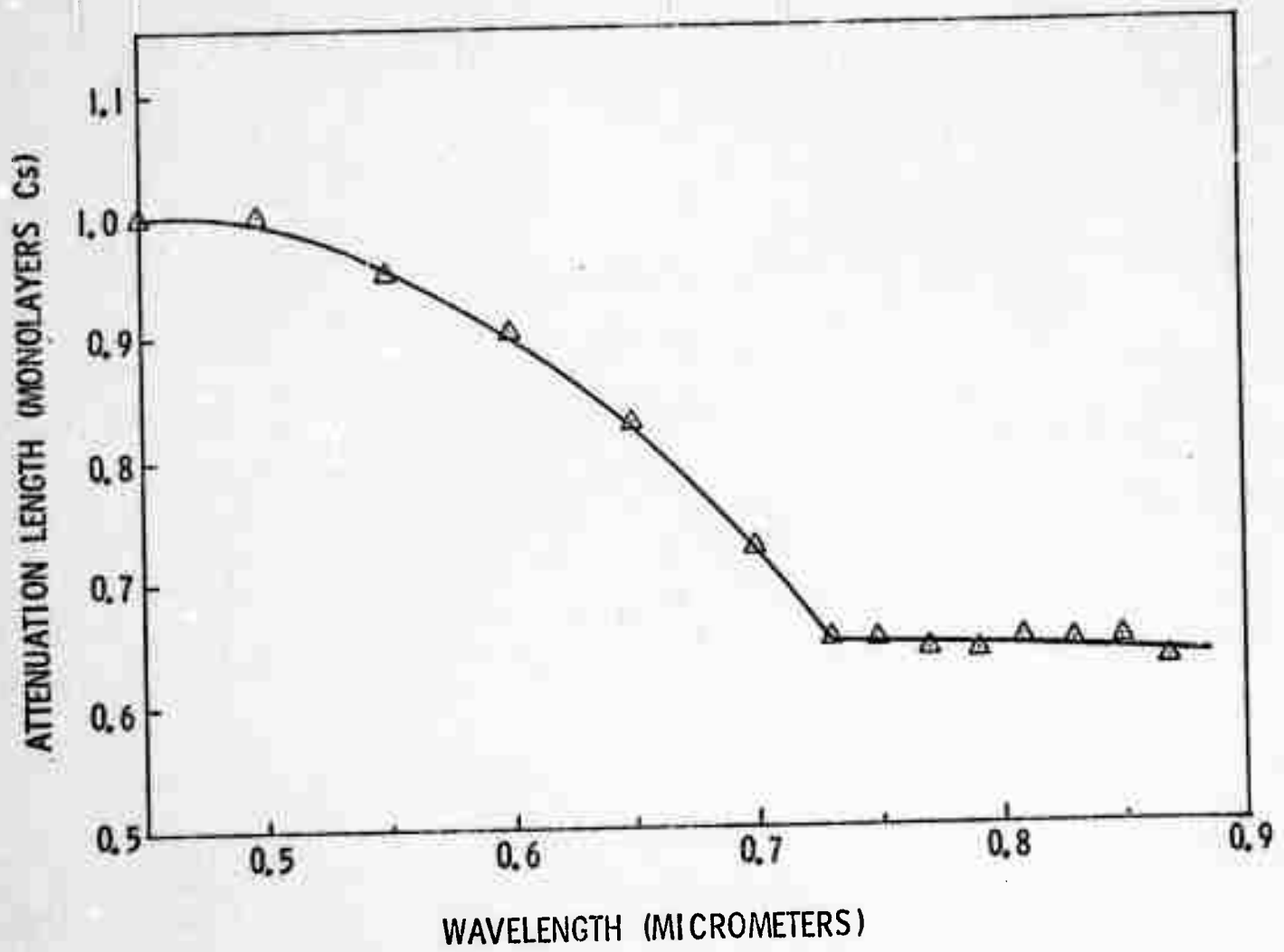


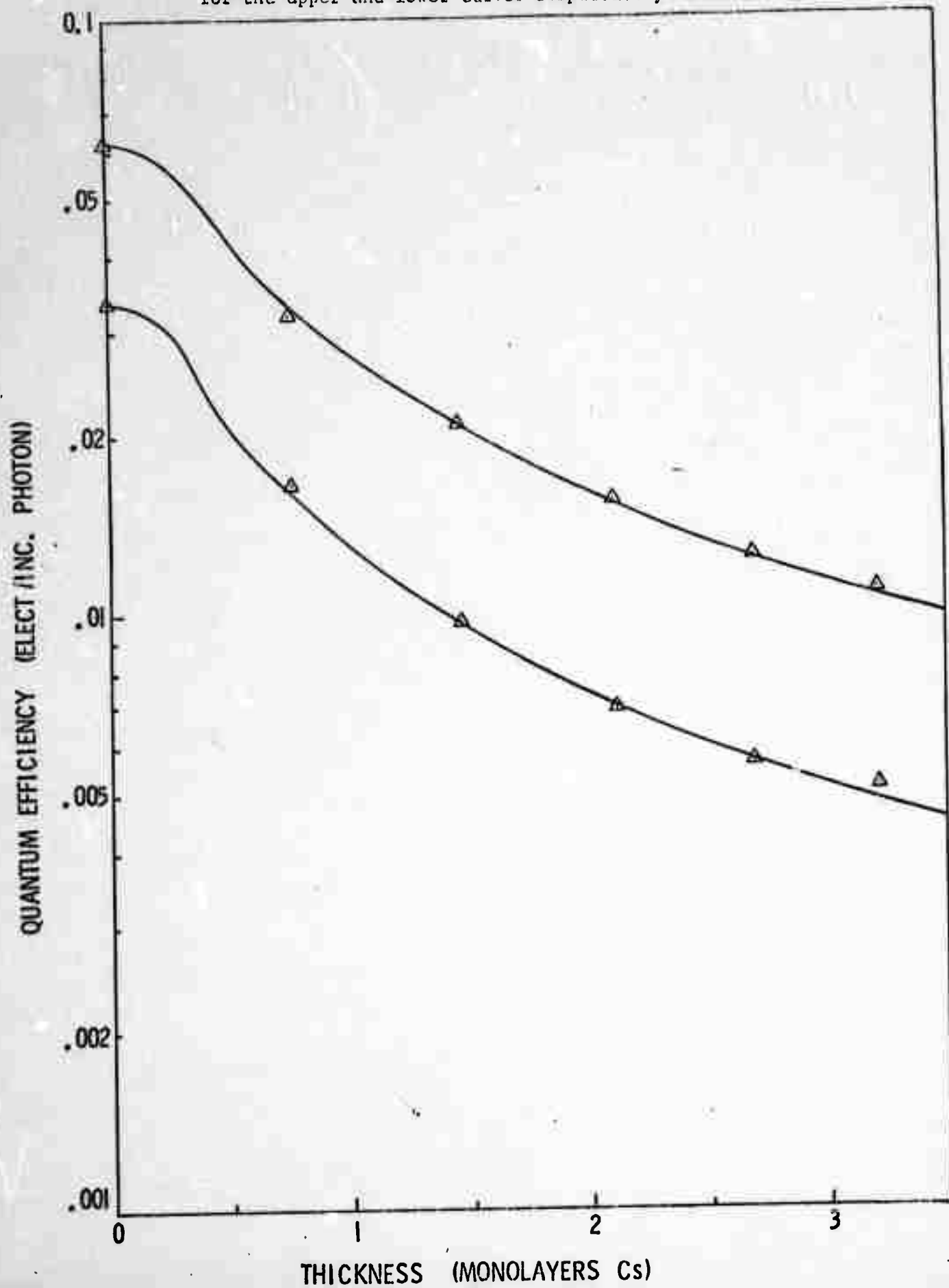
Figure 6 Wavelength dependence of the attenuation length of Cs-0 low-work-function surfaces on GaAs.



We have also verified equation (2) for  $\text{InAs}_{0.4}\text{P}_{0.6}$ . Figure 7 shows the thickness dependence of the yield from  $\text{InAs}_{0.4}\text{P}_{0.6}$  at 0.63 microns (upper curve) and 0.7 microns (lower curve). The points on the curves are the actual data points, and the solid line represents equation (2) with  $\eta_0 = 0.062$  and  $\ell = 0.6$  for the upper curve, and  $\eta_0 = 0.0335$  and  $\ell = 0.5$  for the lower curve.

If, as in reference 1, we assume that the sticking coefficient of  $C_s$  on  $\text{InAs}_{0.4}\text{P}_{0.6}$  and on GaAs does not change significantly with coverage,<sup>(13)</sup> then the Cs-0 low-work-function surface in an infrared-optimized  $\text{InAs}_{0.4}\text{P}_{0.6}$  cathode is approximately 2.3 monolayers of Cs thicker than that of optimized GaAs. From equation 2, with  $\ell = 0.65$  monolayers, we find that an additional 2.3 monolayers of Cs would reduce the infrared photoresponse of GaAs by a factor of about 4. We do not have sufficient data on  $\text{InAs}_{0.4}\text{P}_{0.6}$  to allow us to determine its attenuation length near threshold, however from Figure 7, we expect that it will be smaller than 0.65 monolayers. Consequently alone on the basis of the increased thickness required to optimize the infrared response of  $\text{InAs}_{0.4}\text{P}_{0.6}$ , we would expect the threshold response of  $\text{InAs}_{0.4}\text{P}_{0.6}$  to be lower than that of GaAs by a factor of 5 or more<sup>(14)</sup>.

Figure 7 Thickness dependance of the quantum efficiency  $\eta$  of  $\text{InAs}_{0.4}\text{P}_{0.6}$  at  $6300\text{\AA}$  (upper curve) and  $7000\text{\AA}$  (lower curve). The points represent the experimental data and the solid curves are plots of the equations  $\eta = 0.062(1 - e^{-0.6/t})$  and  $\eta = 0.0335(1 - e^{-0.5/t})$  for the upper and lower curves respectively.



## REFERENCES

1. H. Sonnenberg, Appl. Phys. Lett 19, 431 (1971).
2. A monolayer of Cs is defined here as the amount of Cs required to optimize the photoresponse at  $6328\text{\AA}$  with Cs only.
3. We assume that the Cs and  $\text{O}_2$  sticking coefficients do not change significantly with coverage.
4. The fact that T is greater than 1 shows that some  $\text{O}_2$  is required to optimize the photoresponse at all wavelengths, including the ultra violet range.
5. Note that the efficiency at 1.3 microns is almost 0.02%. Further improvement with better  $\text{InAs}_{0.4}\text{P}_{0.6}$  material can be expected.
6. If we make the same assumptions about the Cs-O surface that were made in reference 1, we find that the low-work-function surface consists of approximately 1 monolayer of Cs and 1.7 monolayers of  $\text{Cs}_2\text{O}$ .
7. L. W. James and J. J. Uebbing, Appl. Phys. Letters 16, 370 (1970).
8. R. L. Bell, L. W. James, G. A. Antypas, J. Edgecumbe, and R. L. Moon, Appl. Phys. Letters 19, 513 (1971).
9. The ratio of Cs to  $\text{O}_2$  remains constant.
10. L. W. James and J. L. Moll Phys. Rev. 183, 740 (1969).
11. High escape probabilities such as this were achieved with  $\langle 110 \rangle$  GaAs surfaces. Our best yield curves obtained in this material are comparable to those obtained on  $\langle 111\text{B} \rangle$  GaAs by L. W. James, G. A. Antypas, J. Edgecumbe, R. L. Moon, and R. L. Bell, J. of Appl. Phys. 42, 4976 (1971). Our yield is slightly better than theirs above 1.65 eV but slightly lower than theirs below about 1.6 eV. The decreased yield in the infrared is probably due to the low doping of our material ( $1 \times 10^{18} \text{cm}^{-3}$ ).
12. L. W. James, J. L. Moll, and W. E. Spicer Symposium on GaAs, 230, (1968).

13. The fact that the setting of the Cs channel at the point of equilibrium (Cs loss = Cs gain) remains essentially the same at all exposure levels, seems to confirm that the assumption is valid.
14. Since the thickness of the low-work-function surface has such a profound effect on photoemission, it is not surprising that a great deal of progress in the processing of infrared cathodes has recently been made.